Journal of Molecular Evolution (2020) 88:501–509
https://doi.org/10.1007/s00239-020-09945-1

ORIGINAL ARTICLE

G:U-Independent RNA Minihelix Aminoacylation by *Nanoarchaeum equitans* Alanyl-tRNA Synthetase: An Insight into the Evolution of Aminoacyl-tRNA Synthetases

Misa Arutaki[1] · Ryodai Kurihara[1] · Toru Matsuoka[1] · Ayako Inami[1] · Kei Tokunaga[1] · Tomomasa Ohno[1] · Hiroki Takahashi[1] · Haruka Takano[1] · Tadashi Ando[2,3] · Hiromi Mutsuro-Aoki[1] · Takuya Umehara[1] · Koji Tamura[1,3]

Received: 25 December 2019 / Accepted: 28 April 2020 / Published online: 7 May 2020

Abstract

Nanoarchaeum equitans is a species of hyperthermophilic archaea with the smallest genome size. Its alanyl-tRNA synthetase genes are split into AlaRS-α and AlaRS-β, encoding the respective subunits. In the current report, we surveyed *N. equitans* AlaRS-dependent alanylation of RNA minihelices, composed only of the acceptor stem and the T-arm of $tRNA^{Ala}$. Combination of AlaRS-α and AlaRS-β showed a strong alanylation activity specific to a single G3:U70 base pair, known to mark a specific tRNA for charging with alanine. However, AlaRS-α alone had a weak but appreciable alanylation activity that was independent of the G3:U70 base pair. The shorter 16-mer RNA tetraloop substrate mimicking only the first four base pairs of the acceptor stem of $tRNA^{Ala}$, but with C3:G70 base pair, was also successfully aminoacylated by AlaRS-α. The end of the acceptor stem, including CCA-3′ terminus and the discriminator A73, was able to function as a minimal structure for the recognition by the enzyme. Our findings imply that aminoacylation by *N. equitans* AlaRS-α may represent a vestige of a primitive aminoacylation system, before the appearance of the G3:U70 pair as an identity element for alanine.

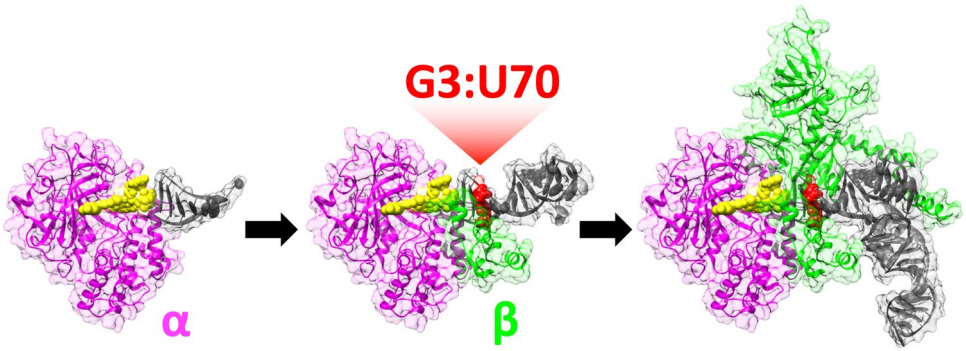

Keywords tRNA · Minihelix · Alanyl-tRNA synthetase · *Nanoarchaeum equitans* · G3:U70 independent aminoacylation · Evolution

Introduction

Aminoacyl-tRNA synthetases (aaRSs) play a central role in protein biosynthesis. Accurate primary protein sequences are assured by the proper attachment of cognate amino acids to their corresponding cognate tRNAs catalyzed by aaRSs (Schimmel 1987; Schimmel and Söll 1979). The aminoacylation reaction is generally performed by the activation of an amino acid (aminoacyl adenylate formation), followed

Handling editor: **Ramanarayanan Krishnamurthy**.

Misa Arutaki and Ryodai Kurihara have contributed equally to this work.

Extended author information available on the last page of the article

by the transfer to a cognate tRNA. (Arginyl-, glutaminyl-, glutamyl-, and class I lysyl-tRNA synthetases require the presence of tRNA for amino acid activation (Schimmel and Söll 1979; Ibba et al. 1999).) To ensure accurate assignment, each aaRS recognizes specific regions of their corresponding tRNA. These identity elements have been extensively investigated. $tRNA^{Ala}$ possesses a unique wobble base pair in the acceptor stem (G3:U70) and this position has been identified as a crucial identity element for recognition by alanyl-tRNA synthetase (AlaRS) (Hou and Schimmel 1988; McClain and Foss 1988). AlaRS is a class II aminoacyl-tRNA synthetase with characteristic antiparallel β-sheets and three conserved sequence motifs (Eriani et al. 1990; Ibba and Söll 2000). The crystal structures of AlaRS from the archaeon *Archaeoglobus fulgidus*, in complex with $tRNA^{Ala}$ have been solved. These structures showed Asp450 and Asn359 in AlaRS (corresponding to Asp400 and Asn303 in *Escherichia coli* AlaRS, respectively) interacting with the amino group at position 2 of G3, and the carbonyl oxygen at position 4 of U70, respectively (Naganuma et al. 2014).

Nanoarchaeum equitans is a species of hyperthermophilic archaea with the smallest genome size (Huber et al. 2002). Some of tRNA- and protein-encoding genes of this archaeon, including the AlaRS gene, are split (Randau et al. 2005a, b; Waters et al. 2003). The genes for the two subunits of AlaRS are separated by half of the chromosome (Waters et al. 2003). Recently, in other members of the Nanoarchaeota phylum, i.e., *Nanobsidianus stetteri* (Nst1) (Wurch et al. 2016), *Nanopusillus acidilobi* (Wurch et al. 2016), and *Nanoclepta minutus* (St John et al. 2019), gene splitting of AlaRS has been estimated. In a previous study using the *N. equitans* AlaRS, a combination of both the subunits (α- and β-chains) of AlaRS was found to be active, but each individual subunit was not active when present alone (Waters et al. 2003). However, as the alanylation assay was performed using *Methanococcus jannaschii* $tRNA^{Ala}$, the target sequence of tRNA was not identical in a strict sense.

The multisequence alignment of *N. equitans* AlaRS-α with *E. coli* AlaRS shows that AlaRS-α almost entirely corresponds to *E. coli* AlaRS368N, a N-terminal fragment with 368 residues of *E. coli* AlaRS (Fig. 1 and Supplementary Material, Fig. S1). Previous studies have shown that the *E. coli* AlaRS368N cannot alanylate $tRNA^{Ala}$ (Jasin et al. 1983; Regan et al. 1987; Chihade and Schimmel 1999), and indeed the minimal *E. coli* AlaRS variant with alanylation activity is the N-terminal 442-residue fragment (AlaRS442N) (Fig. 1 and Supplementary Material, Fig. S1) (Guo et al. 2009).

Minihelices (the coaxial stack of the acceptor stem on the T-arm of the tRNA) have been shown to function as substrates of many aaRSs (Francklyn and Schimmel 1989; Frugier et al. 1994; Martinis and Schimmel 1997; Musier-Forsyth and Schimmel 1999). Similarly, oligonucleotide substrates based on the acceptor stem of $tRNA^{Ala}$ (microhelix) (Francklyn et al. 1992), or a shortened acceptor stem containing a G3:U70 base pair (Shi et al. 1992), are also aminoacylated by AlaRS. Evidence suggests that the top half of the L-shaped tRNA structure may have appeared in evolution prior to the addition of the other half of the structure, which includes the anticodon (Schimmel et al. 1993; Schimmel and Ribas de Pouplana 1995; Tamura 2015). The split forms of the *N. equitans* AlaRS may therefore be connected with the evolutionary history of aaRS enzyme activity.

In this report, we show a very important fact that might be closely related to the evolution of aminoacyl-tRNA synthetases: *N. equitans* AlaRS-α shows the G3:U70 base pair-independent aminoacylation of RNA minihelices with alanine. Our data support the existence of a simplified aminoacylation of $tRNA^{Ala}$ by AlaRS early in the evolutionary process, prior to the appearance of the G3:U70 base pair.

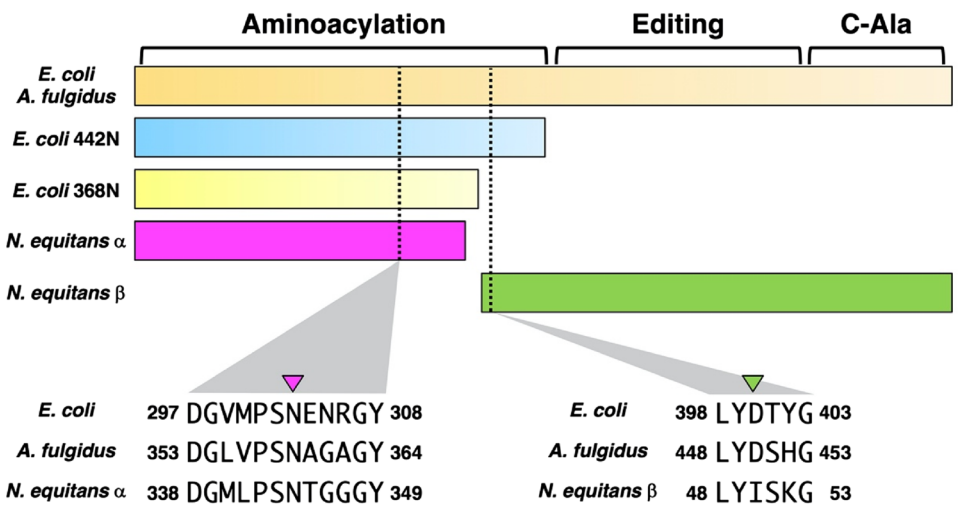

Fig. 1 Schematic diagram of *E. coli*, *A. fulgidus*, and *N. equitans* AlaRS (α and β) sequences. The Asn (N) and Asp (D) residues involved in G3:U70 recognition in *E. coli* and *A. fulgidus* AlaRS are indicated with the amino acid context shown (multisequence alignment of these AlaRSs are given in Supplementary Material, Fig. S1)

Materials and Methods

Plasmid Construction

The coding sequences for AlaRS-α (NEQ547) and AlaRS-β (NEQ211) of *N. equitans* were PCR-amplified from genomic DNA of *N. equitans* (a gift from Dr. Harald Huber, Universität Regensburg, Germany) using the pairs of primers 5′-CAAAAATTCATATGGTTAAAG-3′ and 5′-GATAAC ATGGATCCCGCAAAAAG-3′ for AlaRS-α, and 5′-GTT TTTAGATTCATATGATACC-3′ and 5′-CAATTGTGG ATCCTTTTATAACAAAC-3′ for AlaRS-β. These primers were synthesized by Eurofins Genomics K.K. (Tokyo, Japan). After digestion by *Nde*I and *Bam*HI, the fragments were first incorporated into pET11a (Novagen, Madison, WI), and then the *Nde*I- and *Blp*I-digested fragments were finally transferred into pET15b (Novagen, Madison, WI), to facilitate the purification of the expressed proteins using a 6×His encoding tag at the N-terminus. The DNA sequences were confirmed by Eurofins Genomics K.K. (Tokyo, Japan).

Expression and Purification of *N. equitans* AlaRS-α and AlaRS-β

Escherichia coli BL21-Codon Plus(DE3)-RIL (Stratagene, La Jolla, CA) containing the *N. equitans* AlaRS-α or AlaRS-β were grown and induced with 0.5 mM isopropyl-*β*-D-thiogalactoside (IPTG), respectively. Cultures were harvested and cells were suspended in lysis buffer (20 mM Tris–HCl (pH 8.0), 300 mM NaCl, 10 mM imidazole), followed by the disruption of the cells by sonication on ice. The supernatant was collected after centrifugation and heated to 80 °C for 30 min and re-centrifuged. The supernatant was charged onto a Ni–NTA agarose (QIAGEN, Valencia, CA, USA) column equilibrated with lysis buffer and washed with wash buffer (20 mM Tris–HCl (pH 8.0), 300 mM NaCl, and 20 mM imidazole), and His-tagged AlaRS was eluted with elution buffer (20 mM Tris–HCl (pH 8.0), 300 mM NaCl, and 250 mM imidazole). Fractions containing a homogeneous protein enzyme were pooled and dialyzed twice in 1 L of dialysis buffer [40 mM Tris–HCl (pH 8.0), 200 mM NaCl, 0.2 mM EDTA] followed by concentration by Amicon Ultra Ultracel-30K (Merck Millipore, Billerica, MA, USA). Finally, the enzymes were stored in 50% glycerol.

Preparation of RNA Substrates

Chemically synthesized and/or PCR-amplified DNAs carrying the T7 promoter and the sequences corresponding to *N. equitans* $tRNA^{Ala}$, or $minihelix^{Ala}$ and its mutants were used for RNA transcription. The in vitro transcripts were prepared in a reaction mixture containing 40 mM Tris–HCl (pH 8.0), 8 mM $MgCl_2$, 2 mM spermidine, 1 mM dithiothreitol, 4 mM each NTP, 40 mM 5′GMP, template DNA (~0.2 mg/ml) using T7 RNA polymerase (Sampson and Uhlenbeck 1988; Hamachi et al. 2013). The transcripts were purified by denaturing 12% polyacrylamide gel electrophoresis. The concentrations of purified obtained RNA were determined from the UV absorbance at a wavelength of 260 nm using Implen NanoPhotometer (München, Germany). RNA tetraloop substrate was synthesized by Eurofins Genomics K.K. (Tokyo, Japan). Periodate oxidation of the 3′-terminal adenosine residue of $minihelix^{Ala}$ for generating 2′,3′-dialdehydes was performed using the method reported by Watanabe and coworkers (Kurata et al. 2003). Briefly, the reaction was performed for 60 min at 0 °C in the dark containing 10 mM $NaIO_4$ and the total RNA was recovered by ethanol precipitation.

Aminoacylation Assay

The aminoacylation reaction was performed at 60 °C in a reaction mixture containing 50 mM HEPES–NaOH (pH 7.4), 10 mM $MgCl_2$, 30 mM KCl, 2 mM dithiothreitol, 2 mM ATP and 10 μM L-[U–^{14}C]alanine (132.0 mCi/mmol) (Moravek, Inc., Brea, CA, USA), with 15 μM RNA transcripts and either with [1] 0.5 μM AlaRS-α and 0.5 μM AlaRS-β, or [2] 0.5 μM AlaRS-α, or [3] 0.5 μM AlaRS-β, or [4] 5 μM AlaRS-α, or [5] 5 μM AlaRS-β. Aliquots were removed at specified time points, spotted onto trichloroacetic acid-soaked filter pads, washed with cold 5% trichloroacetic acid, and measured by scintillation counting (Schreier and Schimmel 1972). Kinetic parameters were determined by a Lineweaver–Burk plot of 1/v against 1/[S] ([S] is the RNA concentration and v is the observed initial velocity of alanylation) using various concentrations of RNA and proper concentrations of the enzymes that produce linear initial velocities (Table 1 and Supplementary Material, Fig. S2).

Results

Alanylation Activity of *N. equitans* AlaRS Toward $tRNA^{Ala}$ and $Minihelix^{Ala}$

Although *N. equitans* grows at 80 °C (Huber et al. 2002), alanylation assays were performed at 60 °C to minimize evaporation of the reaction solution during the measurement. We first performed the alanylation assays using a combination of enzymes composed of [1] both AlaRS-α and AlaRS-β, or [2] AlaRS-α alone, or [3] AlaRS-β alone on the $minihelix^{Ala}$, which is made up of the acceptor stem on the T-arm of $tRNA^{Ala}$ (Fig. 2a). At a concentration of 0.5 μM enzyme, $minihelix^{Ala}$ was aminoacylated with the combination of

enzymes containing AlaRS-α and AlaRS-β, but not with either AlaRS-α alone or with AlaRS-β alone (Fig. 3a). However, an increase in the concentration of AlaRS-α to 5 μM resulted in an apparent alanylation activity, whereas 5 μM AlaRS-β did not show any measurable activity (Fig. 3b). A combination of AlaRS-α and AlaRS-β was also active on $tRNA^{Ala}$ and the kinetic parameters of aminoacylation for both on $tRNA^{Ala}$ and the $minihelix^{Ala}$ substrates were similar

Table 1 Kinetic parameters for aminoacylation of $tRNA^{Ala}$ and $minihelix^{Ala}$ by *N. equitans* AlaRS

AlaRS-α + AlaRS-β	k_{cat} (s^{-1})	K_m (μM)	k_{cat}/K_m ($\mu M^{-1}\ s^{-1}$)	k_{cat}/K_m (relative)
$tRNA^{Ala}$	3.0 ± 0.36	1.6 ± 0.067	1.9 ± 0.31	1
$Minihelix^{Ala}$	1.9 ± 0.46	2.1 ± 0.42	0.9 ± 0.44	0.47
AlaRS-α	k_{cat} (s^{-1})	K_m (μM)	k_{cat}/K_m ($\mu M^{-1}\ s^{-1}$)	k_{cat}/K_m (relative)
$tRNA^{Ala}$	0.021 ± 0.0021	7.7 ± 0.93	0.0027 ± 0.00059	1
$Minihelix^{Ala}$	0.028 ± 0.00050	23 ± 1.6	0.0012 ± 0.00030	0.44

The data represent the mean of triplicate experiments ± SEM

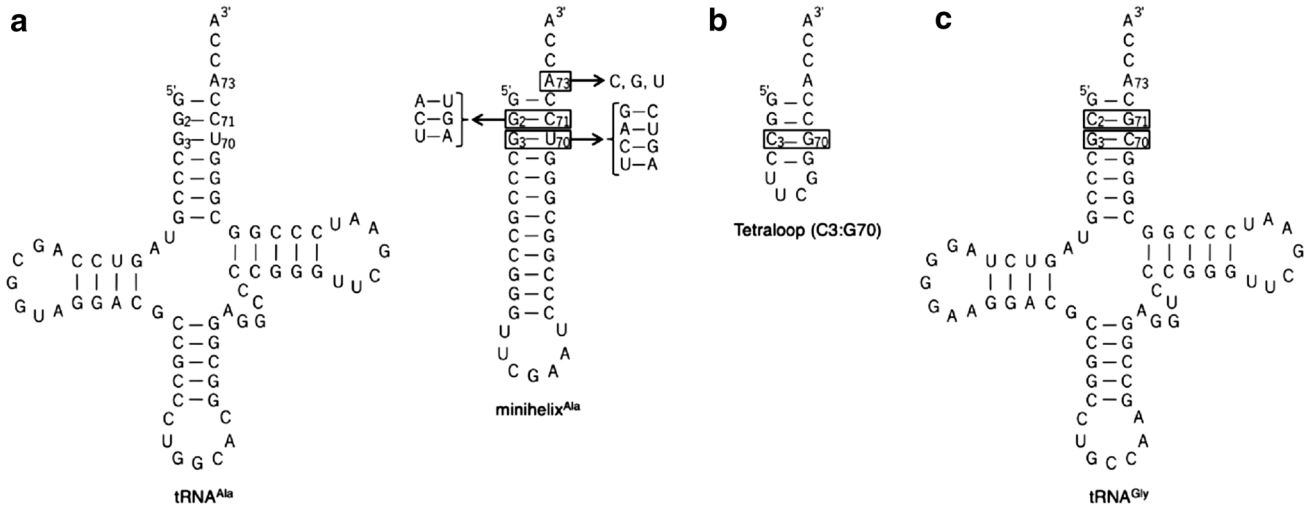

Fig. 2 **a** Sequence of *N. equitans* $tRNA^{Ala}$ (*Left*) and $minihelix^{Ala}$ (*Right*). Numbering is based on that for wild type $tRNA^{Ala}$. $Minihelix^{Ala}$ comprises the acceptor stem and the T-arm of the $tRNA^{Ala}$. Arrows indicate the substitutions performed in this study. **b** Sequence of 16-mer RNA tetraloop substrate including only the first four base pairs of the acceptor stem of $tRNA^{Ala}$, but with C3:G70 base pair. **c** Sequence of *N. equitans* $tRNA^{Gly}$

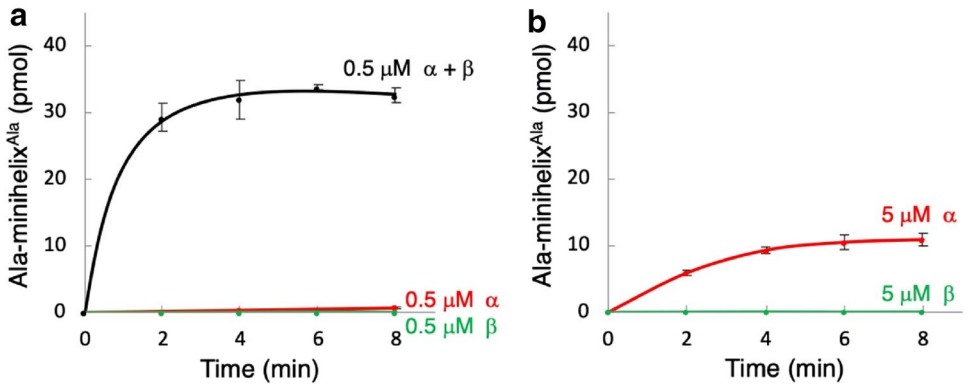

Fig. 3 **a** Alanylation of 15 μM $minihelix^{Ala}$ by the mixture of 0.5 μM AlaRS-α and AlaRS-β, by 0.5 μM AlaRS-α, and by 0.5 μM AlaRS-β. **b** Alanylation of 15 μM of $minihelix^{Ala}$ by 5 μM AlaRS-α and by 5 μM AlaRS-β. Error bars represent the SEM of triplicate experiments

(Table 1). In the case of using AlaRS-α alone, the kinetic parameters of aminoacylation of minihelix^{Ala} was also nearly comparable to those of tRNA^{Ala} (Table 1).

Alanylation Activity of AlaRS on Minihelix^{Ala} Mutants

The unexpected new result that AlaRS-α alone caused the alanylation activity led us to survey the role of G3:U70 of minihelices in aminoacylation by AlaRS-α as well as by the wild-type system composed of both AlaRS-α and AlaRS-β. We created four mutants with Watson–Crick base pairing at position 3–70 (A3:U70, G3:C70, C3:G70, and U3:A70), and assayed their alanylation activities. All G3:U70 mutants tested decreased the aminoacylation activity of 15 μM substrate using 0.5 μM of both AlaRS-α and AlaRS-β, (Fig. 4a). This is consistent with previous data showing that the G3:U70 base pair of tRNA^{Ala} is a major identity element by AlaRS (Hou and Schimmel 1988; McClain and Foss 1988). However, using 5 μM AlaRS-α, G3:C70 mutation had little effect on alanylation compared to the wild-type minihelix^{Ala} (Fig. 4b). Interestingly, the three remaining mutants (A3:U70, C3:G70, and U3:A70) showed higher level of activities compared with the wild-type minihelix^{Ala} (Fig. 4b). We also investigated the alanylation activity using an RNA tetraloop substrate. The tetraloop substrate was synthesized on the basis of the UUCG tetraloop (Tuerk et al. 1988; Woese et al. 1990) and the first four base pairs of the acceptor stem of tRNA^{Ala} (Shi et al. 1992), but the third base pair (G3:U70) was replaced with C3:G70 (Fig. 2b). AlaRS-α aminoacylated the RNA tetraloop substrate (Fig. 4b). Of the three mutants with Watson–Crick base pairing at position 2–71 (A2:U71, C2:G71, and U2:A71), only U2:A71 mutant showed wild-type levels of alanylation (Fig. 4c). A2:U71 and C2:G71 showed reduced activities (Fig. 4c). Finally, we examined the effect of the discriminator A73 substitution on alanylation of minihelix^{Ala}. Substitution of A73 with any other nucleotides caused a significant decrease in alanylation activity (Fig. 4d).

Confirmation for Excluding Artifacts in the Aminoacylation by *N. equitans* AlaRS-α

In order to confirm that other factors did not contribute to the observed charging, we further monitored the reaction. To confirm that aminoacylation occurred at the 3′-end, the minihelix^{Ala} was pre-treated with $NaIO_4$ to oxidize *cis*-hydroxyl groups (Kurata et al. 2003). No aminoacylation was detected in the reaction using *N. equitans* AlaRS-α (Fig. 5). In addition, the controls without any addition of enzyme or RNA did not cause alanylation (Fig. 5). Then, we studied whether AlaRS-α could alanylate tRNA^{Gly} to provide evidence that

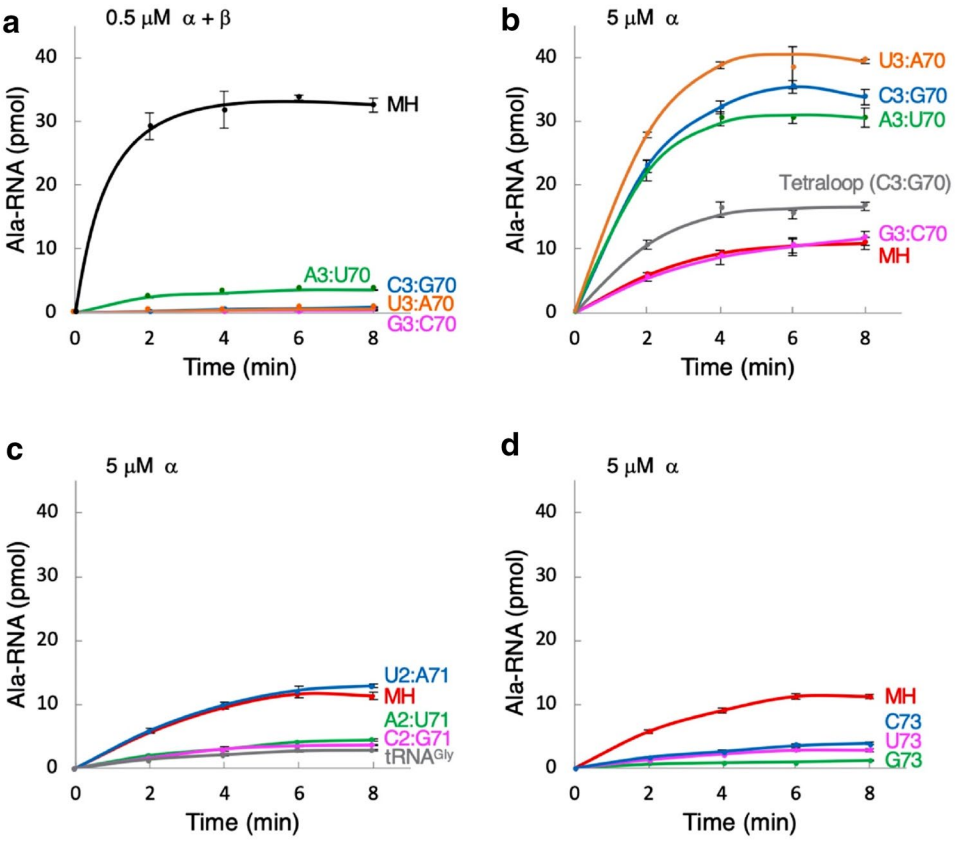

Fig. 4 **a** Alanylation of wild-type minihelix^{Ala} (MH) and its mutants at positions 3–70 by the mixture of 0.5 μM AlaRS-α and AlaRS-β. **b** Alanylation of MH, its mutants at positions 3–70, and the RNA tetraloop substrate shown in Fig. 2b by 5 μM AlaRS-α. **c** Alanylation of MH, its mutants at positions 2–71, and tRNA^{Gly} by 5 μM AlaRS-α. **d** Alanylation of MH and its mutants at position 73 by 5 μM AlaRS-α. The concentration of RNA substrates was 15 μM. Error bars represent the SEM of triplicate experiments

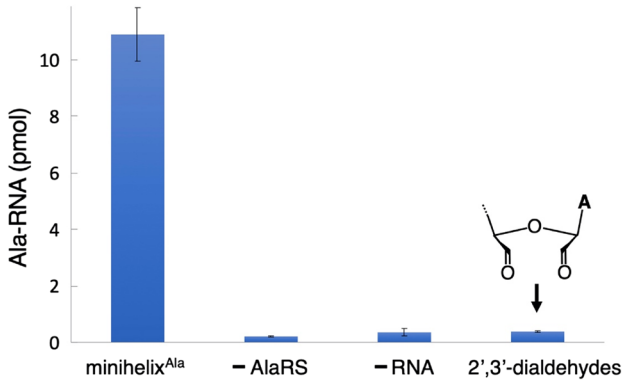

Fig. 5 A comparative study of the aminoacylation reaction. From left to right: minihelix^{Ala} with AlaRS-α (minihelix^{Ala}), minihelix^{Ala} without AlaRS-α (-AlaRS), no minihelix^{Ala} with AlaRS-α (-RNA), and periodate-oxidized minihelix^{Ala} with AlaRS-α (2′,3′-dialdehydes). The scintillation count values after 8 min were used for comparison purposes. All reactions were performed with/without 15 µM of RNA substrates and 5 µM AlaRS-α. Error bars represent the SEM of triplicate experiments

alanylation by AlaRS-α was not dependent on G3:U70 at the tRNA level. *N. equitans* tRNA^{Gly} has a sequence similarity with the tRNA^{Ala} despite the presence of C2:G71 and G3:C70 (Fig. 2c). Previously, we solved the X-ray crystallographic structure of *N. equitans* glycyl-tRNA synthetase (GlyRS), and by performing mutational analysis of the discriminator base A73 and the second base-pair (C2:G71) present on the acceptor stem of tRNA^{Gly}, we elucidated the importance of these positions as key identity elements for the recognition by GlyRS (Fujisawa et al. 2019). tRNA^{Gly} was alanylated by *N. equitans* AlaRS-α to a level comparable to that of the minihelix^{Ala} mutant with C2:G71 (Fig. 4c).

Discussion

The unique G3:U70 base pair in the acceptor stem of tRNA^{Ala} has been shown to be a critical recognition site by AlaRS (Hou and Schimmel 1988; McClain and Foss 1988). Although many aaRSs specifically recognize the anticodons of the corresponding cognate tRNAs, the primordial genetic code is likely to have resided in the minihelix region as the modern tRNA-aaRS system is thought to have evolved from a primordial tRNA-aaRS system (Schimmel et al. 1993; Schimmel and Ribas de Pouplana 1995; Tamura 2015). Although we observed a higher aminoacylation activity in the condition involving a combination of AlaRS-α and AlaRS-β than that observed in a condition with AlaRS-α alone, our data supported two proposed features of the evolution of AlaRS: [1] *N. equitans* AlaRS behaves in a G3:U70 dependent manner when both AlaRS-α and AlaRS-β are present, and [2] *N. equitans* AlaRS-α alone can alanylate tRNA^{Ala} and minihelix^{Ala}, but it behaves in a G3:U70 independent manner. In this context, the G3:U70 may be a late-coming "operational RNA code" (Schimmel et al. 1993; Schimmel and Ribas de Pouplana 1995; Carter and Wills 2018), relevant to later alanylation systems incorporating further specificity through evolution of the AlaRS-β subunit.

N. equitans is a species of hyperthermophilic archaea that grows only in co-culture with another archaeon, *Ignicoccus* sp. strain KIN4/I (Huber et al. 2002). The existence of both genes of AlaRS-α and AlaRS-β in *N. equitans* suggests that both AlaRS-α and AlaRS-β function cooperatively in the organism. However, the behavior of AlaRS-α alone may inform our understanding of early evolution. Although *N. equitans* AlaRS-α is homologous to the *E. coli* AlaRS368N (Fig. 1 and Supplementary Material, Fig. S1), the former can alanylate tRNA^{Ala}, but the latter enzyme cannot alanylate (Jasin et al. 1983; Regan et al. 1987; Chihade and Schimmel 1999). In *E. coli* AlaRS, the region consisting of the residues 369 to 442 is also necessary to perform this reaction (Guo et al. 2009). Especially, a crucial residue for the recognition of G3 in *E. coli* AlaRS is located at 400th position (Asp400), that has been confirmed by an analysis of the crystal structure of *A. fulgidus* AlaRS (Naganuma et al. 2014).

Further analysis of the sequence alignment in combination with the crystal structures of *A. fulgidus* AlaRS complexed with tRNA^{Ala} (Fig. 6a), suggests that AlaRS residues capable of hydrogen bond-formation with the tRNA are conserved. Asn359 in *A. fulgidus* recognizes the carbonyl oxygen at position 4 of U70 and this Asn is also conserved in *N. equitans* AlaRS-α (Fig. 1 and Supplementary Material, Fig. S1). The sequence LYISKG (LYDSHG in *A. fulgidus*) present in *N. equitans* AlaRS-β is likely important for the recognition of G3 (Fig. 1 and Supplementary Material, Fig. S1) (Naganuma et al. 2014). However, the residue corresponding to Asp450 of *A. fulgidus* AlaRS is Ile in *N. equitans* AlaRS-β (Fig. 1 and Supplementary Material, Fig. S1), and the Ile cannot form hydrogen bond seen in the crystal structure of *A. fulgidus* AlaRS and tRNA^{Ala} (Naganuma et al. 2014). Indeed, the "Asp-plus-Asn" architecture of AlaRSs may select G:U in different unconventional ways depending on the three domains of life (Chong et al. 2018).

In the *A. fulgidus* AlaRS-tRNA^{Ala} (A3:U70) complex, the shifted A3 towards the major groove side finally causes the CCA-3′ region to be folded back into the non-reactive route (Naganuma et al. 2014). By the addition of β-chain to the α-chain of *N. equitans* AlaRS, it is possible that this selection may have occurred in a similar manner. However, the G3:U70 base pair-independent aminoacylation caused by AlaRS-α alone could have been performed by a different mechanism. The increase in alanylation activity in the case of three minihelix^{Ala} mutants with Watson–Crick base pairing at position 3–70 (A3:U70, C3:G70, and U3:A70) may suggest that the stability of the acceptor stem affected the

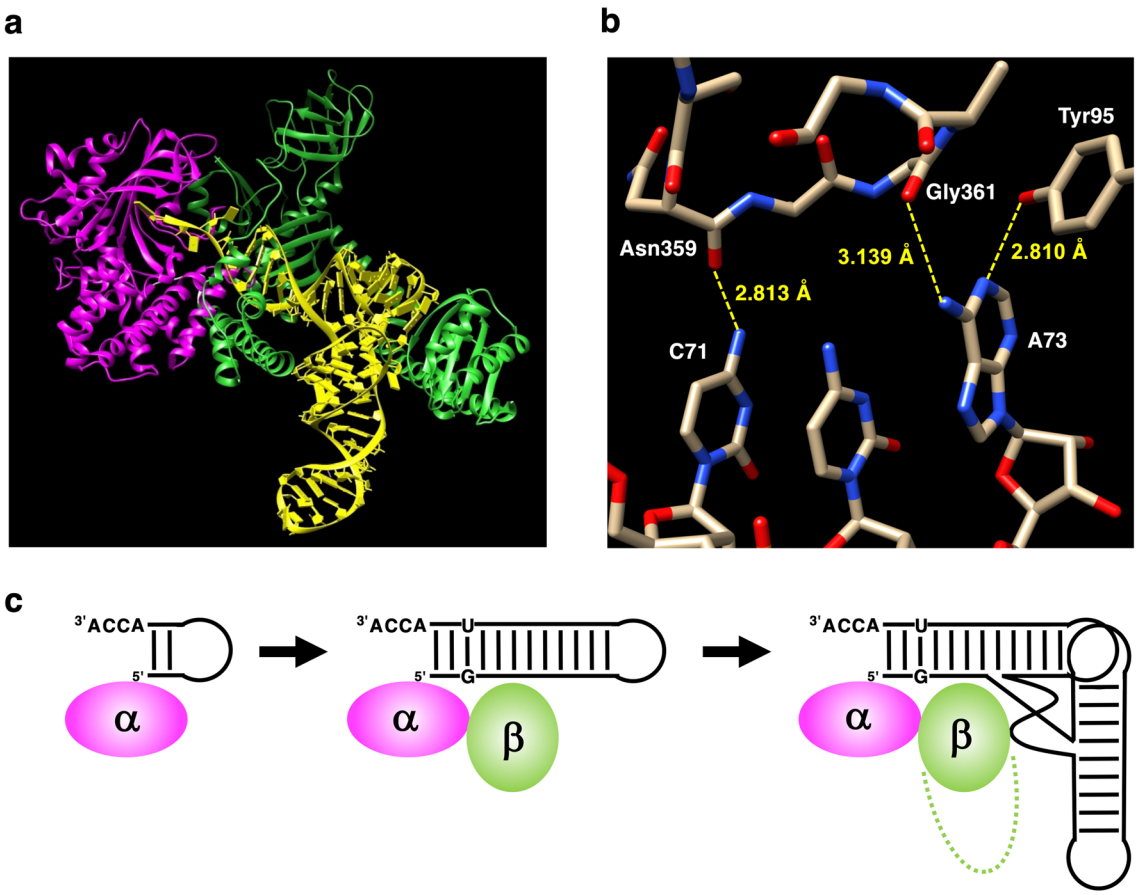

Fig. 6 **a** Tertiary structure of *A. fulgidus* AlaRS complexed with tRNA (PDB ID: 3WQY). The corresponding regions to *N. equitans* AlaRS-α and AlaRS-β are colored in magenta and green, respectively, based on the multisequence alignment (Supplementary Material, Fig. S1). tRNA is shown in yellow. **b** Detailed stick representation of interactions between *A. fulgidus* AlaRS and C71 and A73 of $tRNA^{Ala}$. Distances within 3.5 Å between the amino acid residues of *A. fulgidus* AlaRS and any atoms of C71 and A73 are shown. **c** Schematic simplified representation of the proposed evolutionary processes of AlaRS-$tRNA^{Ala}$ system. Before the appearance of the specific G3:U70, minimalist RNA and protein structures and their interactions resulted in requisite aminoacylation activities (Color figure online)

alanylation potential or that this base pair serves additional unknown roles in the process. Subtle changes could induce a structural effect on the acceptor stem and affect binding of $minihelix^{Ala}$ to the active site of AlaRS-α. Our data using the RNA tetraloop substrate with a C3:G70 base pair (Fig. 2b and Fig. 3b) are quite noteworthy, which strengthens the assertion that the G3:U70 base pair is not important for specific aminoacylation by *N. equitans* AlaRS-α. The thermal melting temperatures of these RNA tetraloop substrates were extensively investigated and they ranged over 70 °C when the discriminator was A (Shi et al. 1992). This could be a possible reason why the RNA tetraloop consisting of a C3:G70 base pair worked as a good substrate with *N. equitans* AlaRS-α at 60 °C (Fig. 2b and Fig. 3b).

In the complex structure of *A. fulgidus* AlaRS-$tRNA^{Ala}$ (Naganuma et al. 2014), the distance between the amino nitrogen at position 6 of A73 and the carbonyl oxygen of Gly361 main chain is 3.14 Å, which may contribute the formation of a hydrogen bond between them (Fig. 6b). In addition, the distance between the nitrogen at position 1 of A73 and the hydroxyl oxygen of Tyr95 is 2.81 Å (Fig. 6b). In our present experiment using *N. equitans* AlaRS-α and $minihelix^{Ala}$ system, the significant decrease in alanylation activity was detected by substitution of A73 with any other nucleotides (Fig. 4d). Although the electron donor–acceptor relationship of these two positions of A73 is the same as that of C73 (positions 4 and 3, respectively), productive interactions may be disrupted by the A73 to C73 mutation due to differences from the glycosyl bond. In the case of the 2–71 mutants, the U2:A71 mutant retained almost the same activity as that of the wild-type $minihelix^{Ala}$ (with G2:C71) (Fig. 4c). In the G2:C71 base pair, the amino group at position 4 of C71 hydrogen-bonds with the carbonyl group at position 6 of G2 in the major groove. In the *A. fulgidus* AlaRS-$tRNA^{Ala}$ complex (Naganuma et al. 2014), the distance between the amino nitrogen and the carbonyl oxygen of

Asn359 main chain is 2.81 Å (Fig. 6b), which allows formation of a hydrogen bond between the amino hydrogen and the carbonyl oxygen. The electron donor–acceptor relationship of the amino group at position 4 of C71 is the same as that of the amino group at position 6 of A71. Therefore, the interaction of the amino hydrogen and the carbonyl oxygen may be retained on G2:C71 to U2:A71 substitution (Fig. 6b).

In summary, our data support a model where *N. equitans* AlaRS-α alone interacts with the end of the acceptor stem and the ACCA-3′ of $tRNA^{Ala}$, but not the G3:U70 base pair (Fig. 6c). This is contrast to prior knowledge regarding $tRNA^{Ala}$ and AlaRS system. Although a specific mechanism of the G3:U70 pair recognition by the protein enzyme is not conserved, the G3:U70 pair as an identity element for alanine is conserved. This suggests that the G3:U70 pair appeared early during genetic code evolution and used as a "second genetic code" (Chong et al. 2018). However, before the appearance of the specific G3:U70, minimalist RNA–protein interactions may have resulted in requisite aminoacylation activities. The activity of AlaRS-α shown in the present study may reflect a vestige of such a primordial aminoacylation of an RNA comprising a small number of nucleotides, including the NCCA-3′ (Fig. 6c). In related to this hypothesis, it is suggested that the G3:U70 base pair recognition is actually a later addition to the original operational code (Carter and Wills 2018), as it is likely implemented by segments of the enzyme that were not accessible to the earliest ancestral aaRS forms (Carter 2014). Furthermore, the genomic tag model proposes that ancient linear RNA genomes possessed tRNA-like structures with a 3′-terminal CCA (Weiner and Maizels 1987). A hairpin RNA with NCCA-3′ has also been proposed as the origin of homochiral aminoacylation in the RNA world (Tamura and Schimmel 2004, 2006; Ando et al. 2018; Tamura 2019). Recently, our in vitro selection study also isolated RNA aptamers composed of 21 nucleotides which bind to a tRNA-binding protein (Trbp) from an extremophile archaeon *Aeropyrum pernix,* and we noticed that the 3′-terminal single stranded CA nucleotides were essential for this binding (Ohmori et al. 2020). The C-terminal domain of methionyl-tRNA synthetase (MetRS-C) from *N. equitans* is homologous to Trbp and the binding of the split 3′-half tRNA with CCA to MetRS-C was stronger than that of the 5′-half tRNA (Suzuki et al. 2017). Extensive investigations using the mutants of *N. equitans* AlaRS-α and structural analysis will be our focus for future study.

Electronic supplementary material The online version of this article (https://doi.org/10.1007/s00239-020-09945-1) contains supplementary material, which is available to authorized users.

Acknowledgements We thank Harald Huber (Universität Regensburg, Germany) for kindly providing genomic DNA of *N. equitans*.

Funding Grants-in Aid for Scientific Research from The Ministry of Education, Culture, Sports, Science and Technology (MEXT), Japan (Grant No. 17K19210 to KT).

Compliance with Ethical Standards

Conflict of interest The authors declare that they have no conflict of interest.

References

Ando T, Takahashi S, Tamura K (2018) Principles of chemical geometry underlying chiral selectivity in RNA minihelix aminoacylation. Nucleic Acids Res 46:11144–11152

Carter CW Jr (2014) Urzymology: experimental access to a key transition in the appearance of enzymes. J Biol Chem 289:30213–30220

Carter CW Jr, Wills PR (2018) Hierarchical groove discrimination by class I and II aminoacyl-tRNA synthetases reveals a palimpsest of the operational RNA code in the tRNA acceptor-stem bases. Nucleic Acids Res 46:9667–9683

Chihade JW, Schimmel P (1999) Assembly of a catalytic unit for RNA microhelix aminoacylation using nonspecific RNA binding domains. Proc Natl Acad Sci USA 96:12316–12321

Chong YE, Guo M, Yang XL, Kuhle B, Naganuma M, Sekine SI, Yokoyama S, Schimmel P (2018) Distinct ways of G: U recognition by conserved tRNA binding motifs. Proc Natl Acad Sci USA 115:7527–7532

Eriani G, Delarue M, Poch O, Gangloff J, Moras D (1990) Partition of tRNA synthetases into two classes based on mutually exclusive sets of sequence motifs. Nature 347:203–206

Francklyn C, Schimmel P (1989) Aminoacylation of RNA minihelices with alanine. Nature 337:478–481

Francklyn C, Shi JP, Schimmel P (1992) Overlapping nucleotide determinants for specific aminoacylation of RNA microhelices. Science 255:1121–1125

Frugier M, Florentz C, Giegé R (1994) Efficient aminoacylation of resected RNA helices by class II aspartyl-tRNA synthetase dependent on a single nucleotide. EMBO J 13:2219–2226

Fujisawa A, Toki R, Miyake H, Shoji T, Doi H, Hayashi H, Hanabusa R, Mutsuro-Aoki H, Umehara T, Ando T, Noguchi H, Voet A, Park SY, Tamura K (2019) Glycyl-tRNA synthetase from *Nanoarchaeum equitans*: the first crystal structure of archaeal GlyRS and analysis of its tRNA glycylation. Biochem Biophys Res Commun 511:228–233

Guo M, Chong YE, Beebe K, Shapiro R, Yang XL, Schimmel P (2009) The C-Ala domain brings together editing and aminoacylation functions on one tRNA. Science 325:744–747

Hamachi K, Hayashi H, Shimamura M, Yamaji Y, Kaneko A, Fujisawa A, Umehara T, Tamura K (2013) Glycols modulate terminator stem stability and ligand-dependency of a glycine riboswitch. BioSystems 113:59–65

Hou YM, Schimmel P (1988) A simple structural feature is a major determinant of the identity of a transfer RNA. Nature 333:140–145
Huber H, Hohn MJ, Rachel R, Fuchs T, Wimmer VC, Stetter KO (2002) A new phylum of Archaea represented by a nanosized hyperthermophilic symbiont. Nature 417:63–67
Ibba M, Losey HC, Kawarabayasi Y, Kikuchi H, Bunjun S, Söll D (1999) Substrate recognition by class I lysyl-tRNA synthetases: a molecular basis for gene displacement. Proc Natl Acad Sci USA 96:418–423
Ibba M, Söll D (2000) Aminoacyl-tRNA synthesis. Annu Rev Biochem 69:617–650
Jasin M, Regan L, Schimmel P (1983) Modular arrangement of functional domains along the sequence of an aminoacyl tRNA synthetase. Nature 306:441–447
Kurata S, Ohtsuki T, Suzuki T, Watanabe K (2003) Quick two-step RNA ligation employing periodate oxidation. Nucleic Acids Res 31:e145
Martinis SA, Schimmel P (1997) Small RNA oligonucleotide substrates for specific aminoacylations. tRNA: Structure, Biosynthesis, and Function. ASM Press, Washington DC, pp 349–370
McClain WH, Foss K (1988) Changing the identity of a tRNA by introducing a G-U wobble pair near the 3′ acceptor end. Science 240:793–796
Musier-Forsyth K, Schimmel P (1999) Atomic determinants for aminoacylation of RNA minihelices and relationship to genetic code. Acc Chem Res 32:368–375
Naganuma M, Sekine S, Chong YE, Guo M, Yang XL, Gamper H, Hou YM, Schimmel P, Yokoyama S (2014) The selective tRNA aminoacylation mechanism based on a single G•U pair. Nature 510:507–511
Ohmori S, Wani M, Kitabatake S, Nakatsugawa Y, Ando T, Umehara T, Tamura K (2020) RNA aptamers for a tRNA-binding protein from *Aeropyrum pernix* with homologous counterparts distributed throughout evolution. Life 10:11
Randau L, Calvin K, Hall M, Yuan J, Podar M, Li H, Söll D (2005a) The heteromeric *Nanoarchaeum equitans* splicing endonuclease cleaves noncanonical bulge-helix-bulge motifs of joined tRNA halves. Proc Natl Acad Sci USA 102:17934–17939
Randau L, Münch R, Hohn MJ, Jahn D, Söll D (2005b) *Nanoarchaeum equitans* creates functional tRNAs from separate genes for their 5′- and 3′-halves. Nature 433:537–541
Regan L, Bowie J, Schimmel P (1987) Polypeptide sequences essential for RNA recognition by an enzyme. Science 235:1651–1653
Sampson JR, Uhlenbeck OC (1988) Biochemical and physical characterization of an unmodified yeast phenylalanine transfer RNA transcribed *in vitro*. Proc Natl Acad Sci USA 85:1033–1037
Schimmel P (1987) Aminoacyl tRNA synthetases: general scheme of structure-function relationships in the polypeptides and recognition of transfer RNAs. Annu Rev Biochem 56:125–158
Schimmel P, Giegé R, Moras D, Yokoyama S (1993) An operational RNA code for amino acids and possible relationship to genetic code. Proc Natl Acad Sci USA 90:8763–8768
Schimmel P, Ribas de Pouplana L (1995) Transfer RNA: from minihelix to genetic code. Cell 81:983–986
Schimmel PR, Söll D (1979) Aminoacyl-tRNA synthetases: general features and recognition of transfer RNAs. Annu Rev Biochem 48:601–648
Schreier AA, Schimmel PR (1972) Transfer ribonucleic acid synthetase catalyzed deacylation of aminoacyl transfer ribonucleic acid in the absence of adenosine monophosphate and pyrophosphate. Biochemistry 11:1582–1589
Shi JP, Martinis SA, Schimmel P (1992) RNA tetraloops as minimalist substrates for aminoacylation. Biochemistry 31:4931–4936
St John E, Liu Y, Podar M, Stott MB, Meneghin J, Chen Z, Lagutin K, Mitchell K, Reysenbach AL (2019) A new symbiotic nanoarchaeote (*Candidatus* Nanoclepta minutus) and its host (*Zestosphaera tikiterensis* gen. nov., sp. nov.) from a New Zealand hot spring. Syst Appl Microbiol 42:94–106
Suzuki H, Kaneko A, Yamamoto T, Nambo M, Hirasawa I, Umehara T, Yoshida H, Park SY, Tamura K (2017) Binding properties of split tRNA to the C-terminal domain of methionyl-tRNA synthetase of *Nanoarchaeum equitans*. J Mol Evol 84:267–278
Tamura K (2015) Origins and early evolution of the tRNA molecule. Life 5:1687–1699
Tamura K (2019) Perspectives on the origin of biological homochirality on Earth. J Mol Evol 87:143–146
Tamura K, Schimmel P (2004) Chiral-selective aminoacylation of an RNA minihelix. Science 305:1253
Tamura K, Schimmel PR (2006) Chiral-selective aminoacylation of an RNA minihelix: mechanistic features and chiral suppression. Proc Natl Acad Sci USA 103:13750–13752
Tuerk C, Gauss P, Thermes C, Groebe DR, Gayle M, Guild N, Stormo G, d'Aubenton-Carafa Y, Uhlenbeck OC, Tinoco I Jr (1988) CUU CGG hairpins: extraordinarily stable RNA secondary structures associated with various biochemical processes. Proc Natl Acad Sci USA 85:1364–1368
Waters E, Hohn MJ, Ahel I, Graham DE, Adams MD, Barnstead M, Beeson KY, Bibbs L, Bolanos R, Keller M, Kretz K, Lin X, Mathur E, Ni J, Podar M, Richardson T, Sutton GG, Simon M, Söll D, Stetter KO, Short JM, Noordewier M (2003) The genome of *Nanoarchaeum equitans*: insights into early archaeal evolution and derived parasitism. Proc Natl Acad Sci USA 100:12984–12988
Weiner AM, Maizels N (1987) tRNA-like structures tag the 3′ ends of genomic RNA molecules for replication: implications for the origin of protein synthesis. Proc Natl Acad Sci USA 84:7383–7387
Woese CR, Winker S, Gutell RR (1990) Architecture of ribosomal RNA: constraints on the sequence of "tetra-loops". Proc Natl Acad Sci USA 87:8467–8471
Wurch L, Giannone RJ, Belisle BS, Swift C, Utturkar S, Hettich RL, Reysenbach AL, Podar M (2016) Genomics-informed isolation and characterization of a symbiotic Nanoarchaeota system from a terrestrial geothermal environment. Nat Commun 7:12115

Authors and Affiliations

Misa Arutaki[1] · Ryodai Kurihara[1] · Toru Matsuoka[1] · Ayako Inami[1] · Kei Tokunaga[1] · Tomomasa Ohno[1] · Hiroki Takahashi[1] · Haruka Takano[1] · Tadashi Ando[2,3] · Hiromi Mutsuro-Aoki[1] · Takuya Umehara[1] · Koji Tamura[1,3]

✉ Koji Tamura
koji@rs.tus.ac.jp

[1] Department of Biological Science and Technology, Tokyo University of Science, 6-3-1 Niijuku, Katsushika-ku, Tokyo 125-8585, Japan

[2] Department of Applied Electronics, Tokyo University of Science, 6-3-1 Niijuku, Katsushika-ku, Tokyo 125-8585, Japan

[3] Research Institute for Science and Technology, Tokyo University of Science, 2641 Yamazaki, Noda, Chiba 278-8510, Japan